The Journal of Experimental Biology 200, 2919–2926 (1997)
Printed in Great Britain © The Company of Biologists Limited 1997
JEB1022

VOLTAGE SENSING IN JELLYFISH *SHAKER* K^+ CHANNELS

NIKITA G. GRIGORIEV, J. DAVID SPAFFORD, WARREN J. GALLIN AND ANDREW N. SPENCER*
Department of Biological Sciences, University of Alberta, Edmonton, Alberta, Canada T6G 2E9 and *Bamfield Marine Station, Bamfield, British Columbia, Canada V0R 1B0*

Accepted 18 August 1997

Summary

The S4 segment of the jellyfish (*Polyorchis penicillatus*) *Shaker* channel jShak1 contains only six positively charged motifs. All other *Shaker* channels, including the jellyfish *Shaker* channel jShak2, have seven charges in this segment. Despite their charge differences, both these jellyfish channels produce currents with activation and inactivation curves shifted by approximately +40 mV relative to other *Shaker* currents.

Adding charge without changing segment length by mutating the N-terminal side of *jShak1* S4 does not have a pronounced effect on channel activation properties. Adding the positively charged motif RIF on the N-terminal side of K294 (the homologue of K374 in *Drosophila Shaker*, which is a structurally critical residue) produced a large positive shift in both activation and inactivation without altering the slope of the activation curve of the channel. When IFR was added to the other side of K294, there was a small negative shift in activation and fast inactivation of the channel was prevented.

Our results demonstrate that K294 divides the S4 segment into functionally different regions and that the voltage threshold for activation and inactivation of the channel is not determined by the total charge on S4.

Key words: *Polyorchis penicillatus*, Hydrozoa, *Shaker* K^+ channels, *jShak1*, *jShak2*, site-directed mutagenesis, S4 segment, voltage sensing, charge, evolution, activation, inactivation, gating valence, threshold.

Introduction

The *Shaker* sub-family of K^+ channel genes appears to be ubiquitous in both invertebrates (Papazian *et al.* 1987; Kamb *et al.* 1987; Tempel *et al.* 1987; Johansen *et al.* 1990; Pfaffinger *et al.* 1991; Kim *et al.* 1995: Jegla *et al.* 1995, Wei *et al.* 1996) and vertebrates (e.g. Baumann *et al.* 1988; Tempel *et al.* 1988). The *Shaker* sub-family is structurally distinct from other members (*Shal*, *Shab* and *Shaw*) of an extended gene family. Two *Shaker* genes, *jShak1* and *jShak2*, recently isolated from the hydrozoan jellyfish *Polyorchis penicillatus* (Phylum Cnidaria) show marked similarity to other *Shaker* sequences (Jegla *et al.* 1995).

A critical structural element of the proposed voltage sensor (S4) of most voltage-gated ion channels is a distinct pattern of repeating motifs of the form Arg-*X*-*X* or Lys-*X*-*X*. It is believed that these positively charged motifs form a structure that senses large electrical fields across the membrane and can lead to channel opening (Noda *et al.* 1984, 1986; Greenblatt *et al.* 1985). The total charge in S4 may influence the steepness of the activation curve (Liman *et al.* 1991; Logothetis *et al.* 1992, 1993) and contribute to the threshold of activation and voltage-sensitivity of the channel (Papazian *et al.* 1991: Logothetis *et al.* 1993). The number of these positively charged motifs varies from four in *Shal* to seven in *Shaker* (Chandy and Gutman, 1995). jShak1 has only six positively charged residues in its S4 segment, whereas in all other *Shaker* sequences, including jShak2, there are seven charges in S4.

When expressed in *Xenopus laevis* oocytes, the jellyfish genes *jShak1* and *jShak2* produce a channel with activation and steady-state inactivation curves that have strong (approximately +40 mV) rightward shifts relative to all other *Shaker* genes (Jegla *et al.* 1995). This shift occurs despite the total charge differences in the S4 segments of jShak1 and jShak2. Recent studies have shown that charges in the S4 segment contribute unequally to the threshold of activation of the channel (Tytgat *et al.* 1993) and to the equivalent gating charge, with different charges moving different distances through the electrical field (Aggarwal and MacKinnon, 1996; Seoh *et al.* 1996; Larsson *et al.* 1996; Mannuzzu *et al.* 1996). Some charges are crucial for the formation of stabilizing electrostatic interactions with negatively charged residues in other segments (Papazian *et al.* 1991, 1995).

To examine the role of charge and segment length in the S4 region of jellyfish *Shaker* channels, we restored the ‘full complement’ of charge to the S4 region of jShak1 by insertions of the motif Arg/Lys-*X*-*X* and by modifying the sequence of the N-terminal side of S4. We have been able to distinguish between the effects of total charge in S4, charge position and length of the segment on the basis of voltage properties. Our

*Author for correspondence (e-mail: aspencer@bms.bc.ca).

results show that a lysine residue stabilizes the S4 segment and divides it into functionally separate regions.

These studies of early metazoan channels, such as the cnidarian channel proteins jShak1 and jShak2, in conjunction with studies of channels from more derived phyla provide us with a broader basis for understanding the critical elements involved in voltage sensing by the S4 segment.

Materials and methods

Mutagenesis and sequencing

Mutations were introduced into the S4 region of *jShak1* using a polymerase chain reaction (PCR)-based technique for introducing insertions and point mutations (Stappert and Kemler, 1992). Sense primers containing appropriate insertions in the S4 region (3–7, Table 1) and an antisense primer complementary to the *jShak1* sequence from positions 1122 to 1145 (2, Table 1) were used to amplify 3′ end fragments from 10 ng of *jShak1* plasmid. In separate reactions, antisense primers containing the same insertions in the S4 region (8–12, Table 1) and an upstream sense primer complementary to the *jShak1* sequence from positions 588 to 607 (1, Table 1) were used to amplify 5′ end fragments from 10 ng of *jShak1* plasmid. The PCR products were gel-purified, and the pairs of PCR products containing complementary overlapping sequence (underlined sequence in Table 1) were used as a combined template in a second PCR reaction with primers 1 and 2 (Table 1).

PCR reactions (25 µl) were carried out with 1:16 diluted recombinant *Pfu* DNA polymerase (Stratagene) and *Taq* polymerase, 20 pmol of each primer, 20 mmol l^{-1} Tris–HCl (pH 8.3 at 20 °C), 25 mmol l^{-1} KCl, 100 µg ml^{-1} gelatin, 50 µmol l^{-1} each of dNTP and 1.5 mmol l^{-1} $MgCl_2$ in 20 thermal cycles (93 °C, 45 s; 55 to 65 °C, 2 min; 72 °C, 2 min) followed by 10 min at 72 °C.

Products from the second PCR reaction were gel-purified, digested with *Hpa*I and *Nsi*I and inserted into *Hpa*I/*Nsi*I-cut *jShak1*, replacing the wild-type *jShak1* sequence between positions 618 and 1102. Ligation reactions were carried out with equimolar amounts of insert and vector fragment in 50 mmol l^{-1} Tris–HCl (pH 7.8), 10 mmol l^{-1} $MgCl_2$, 1 mmol l^{-1} ATP, 50 µg ml^{-1} bovine serum albumin, 20 mmol l^{-1} dithiothreitol and T4 DNA ligase (6 Weiss units, New England Biolabs) in a total volume of 20 µl. 1 µl of the ligation reaction was electroporated (2 mm cuvettes, 2.8 kV) into electrocompetent XL1-Blue bacteria (Stratagene) and plated on LB-ampicillin. Colonies were picked and grown overnight, and plasmid DNA was purified.

The internal primers for making the RIF and QIF mutants (3,4; 8,9; Table 1) and IFR and IFQ mutants (5,6; 10,11; Table 1) contained nine base pair inserts (double-underlining, Table 1) between positions 879 and 880 and between positions 882 and 883, respectively, in *jShak1*; these insertions disrupt a *Pme*I site, so plasmids were screened for the absence of this site. One expected RIF, *Pme*I-resistant clone contained a single base pair error with C in place of T in the eighth position of the insert, providing a unique mutant with insert RIS (AGA ATT TCT) instead of RIF. The RV for SM mutant contained AG in place of CA at positions 846 and 847 in *jShak1* (7, bold type, Table 1), which disrupts a *Mwo*I site, so plasmids were screened for the absence of this site. Large-scale preparations of plasmid DNA were then purified using a silica-based DNA purification method (Hengen, 1995). Double-stranded DNA sequencing of the region of each plasmid prepared by PCR was carried out on a Perkin-Elmer ABI 373A sequencer using an ABI Prism dye-terminator cycle sequencing kit to confirm that the new plasmids contained only the stated mutations.

Expression and recording

Capped mRNAs were prepared by *in vitro* transcription using a T7 mMessage mMachine kit (Ambion). Adult female *Xenopus laevis* were anesthetised in MS 222, and a unilateral incision was made on the dorsal surface of the abdomen to expose the ovary on one side. Mature oocytes (stage V) were

Table 1. *Sequence of the primers used*

Number	Mutant	Orientation	Sequence
1	All	Sense	GCC CGT ATT TGC CCC AAA AG
2	All	Antisense	GCC ATT GAA CCA ACA ATT TGA CCC
3	RIF	Sense	GTG TTT AGA ATT TTT AAA CTA TCG AGA CAT TCC
4	QIF	Sense	GTG TTT CAA ATT TTT AAA CTA TCG AGA CAT TCC
5	IFR	Sense	TTT AAA ATA TTC CGC CTA TCG AGA CAT TCC CGT
6	IFQ	Sense	TTT AAA ATA TTC CAA CTA TCG AGA CAT TCC CGT
7	RV for SM	Sense	GC AGT AAA GGA TCG TTC AG**A G**TG TTA CGC
8	RIF	Antisense	TAG TTT AAA AAT TCT AAA CAC GCG TAA AAC CC
9	QIF	Antisense	TAG TTT AAA AAT TTG AAA CAC GCG TAA AAC CC
10	IFR	Antisense	TAG GCG GAA TAT TTT AAA CAC GCG TAA AAC CC
11	IFQ	Antisense	TAG TTG GAA TAT TTT AAA CAC GCG TAA AAC CC
12	RV for SM	Antisense	GAA CGA TCC TTT ACT GCT ACT TAC

Single- and double-underlining highlights overlapping sequence for sense and antisense primers; double-underlining highlights sequences inserted into *jShak1*.

Residues in bold type are the replaced sequence for *jShak1*.

removed and defolliculated with 2 mg ml^{-1} collagenase (Sigma, Type I) in Ca^{2+}-free ND 96 (96 mmol l^{-1} NaCl, 2 mmol l^{-1} KCl, 1 mmol l^{-1} $MgCl_2$, 5 mmol l^{-1} Hepes-NaOH, pH 7.5) and injected with 50 nl of *in-vitro*-transcribed mRNA at a concentration of 200–400 ng ml^{-1} using a mechanical micro-injector (Drummond Nanoject). Recordings were made after 2 or 3 days at 17–20 °C. The incubation solution was 50 % L15 medium (Sigma) supplemented with 15 μg ml^{-1} gentamycin.

Expressed currents were recorded using two-electrode voltage-clamp. Cushion electrodes were prepared following the method of Schreibmayer *et al.* (1994) with polyacrylamide gel (PAG) replacing agarose. The tips of both the current and voltage electrodes were filled by suction using a pre-filtered (0.2 μm) solution of 3.5 % acrylamide and *N*,*N*-bisacrylamide at a ratio of 29:1, 0.15 % ammonium persulphate and 0.013 % *N*,*N*,*N*′,*N*′-tetramethylethylenediamine (TEMED) in 2 mol l^{-1} KCl. After PAG polymerization, the electrodes were back-filled with 2 mol l^{-1} KCl containing 1 mmol l^{-1} EGTA and 5 mmol l^{-1} Hepes (hemisodium salt). Before recording, electrodes were stored overnight in the back-filling solution. The recording bath solution was ND 96. Oocytes were selected for low levels of expression of endogenous Cl^- current since Cl^- current blockers were not used.

Current data were acquired using a TL-1 DMA interface and PClamp 6.0 software (Axon Instruments). The procedures used to calculate electrical and kinetic properties of expressed currents were as previously described (Jegla *et al.* 1995).

Results

Rationale for the design of mutants

Fig. 1 shows an alignment of the S4 regions of jShak1, jShak2 and *Shaker* B together with the mutations that were made to jShak1. This alignment shows that an Arg-*X*-*X* motif is lacking in jShak1 compared with jShak2 and *Shaker* B. The missing charge can be added either by mutating the sequence of *jShak1* to include an arginine residue or by insertion of an Arg-*X*-*X* motif. Perozo *et al.* (1994) have shown that K374 in *Shaker* B is critical for proper folding, processing and transport of the channel protein. Our alignment indicates that K294 of jShak1 is homologous with K374 of *Shaker* B. Therefore, we

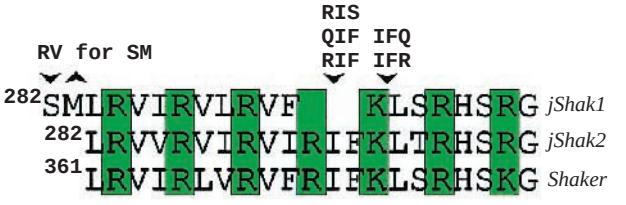

Fig. 1. Manual alignment of the deduced amino acid sequences of the S4 segments of *jShak1*, *jShak2* and *Shaker* B (Jegla *et al.* 1995; Tempel *et al.* 1987). Two types of mutations are shown. Insertions of motifs of three amino acids are shown by ▼, while substitution is shown by ▼▲. Locations of positively charged residues are shown in green.

chose to make one set of insertions (RIF, QIF and RIS) on the N-terminal side of K294, and another set of insertions (IFR and IFQ) on the C-terminal side of K294. RIF, IFR and RIS mutations insert a charged motif and increase the length of the segment, while QIF and IFQ produce the same change in length without adding charge. In addition, the RIS mutant places a hydrophilic residue adjacent to K294. Since the insertion of motifs also increased the total length of the S4 segment, we also made a mutant which added charge without altering total length by mutating the N-terminal sequence of S4 (R for S282 and V for M283). A double substitution was chosen, where valine replaced methionine, in order to keep the relative hydrophobicity of this motif similar to that of the other charged motifs in S4.

All of the mutants, except IFQ, expressed K^+ currents in *Xenopus laevis* oocytes (Fig. 2). Table 2 provides quantitative data on the electrical and kinetic properties of the expressed currents.

Wild type

The wild-type *jShak1* expressed a rapidly inactivating (τ=4.7 ms) K^+ current with a mid-point of activation of +33 mV and an activation slope of 12 mV per e-fold change in conductance (Figs 2A, 3; Table 2). The mid-point of steady-state inactivation (V_{50}) was −28 mV with a slope of 9 mV/e (Fig. 4; Table 2). It is important to note that the values of the mid-points of activation and inactivation reported in this study differ from those reported previously (Jegla *et al.* 1995) when 4,4′-di-isothiocyanatostilbene-2,2′ disulfonic acid (DIDS) was used to block Cl^- currents. We have recently discovered that this substance specifically interferes with the voltage and kinetic properties of jShak1 and jShak2 by unknown mechanisms; however, it does not alter the properties of *Shaker* B. To avoid possible interactions between these blockers and channel function, we did not use Cl^- channel blockers in this study (see Materials and methods).

Substituting RV for SM

When S282 was replaced by R and M283 by V, the resulting mutant produced a current with fast inactivation kinetics (τ=4.4 ms), closely resembling the wild type (Fig. 2B; Table 2). The activation properties (V_{50} +40 mV, slope 12 mV/e) were also similar to those of the wild-type jShak1 (P=0.119, Fig. 3; Table 2), while the steady-state inactivation curve was significantly (P=0.021) shifted in a positive direction (V_{50} −14 mV). The slope of the inactivation curve (6 mV/e) was unchanged from the wild type (Fig. 4; Table 2). Thus, adding a seventh charge by rewriting at the N-terminal end of S4 (SM to RV) does not have pronounced effects on the activation properties of the channel, which contrasts with the other mutants where charge was added by insertion adjacent to K294.

RIF insertion

When RIF was inserted between F293 and K294, this mutant expressed a rapidly inactivating (τ=6.8 ms) K^+ current that had similar kinetic properties to the wild type (Fig. 2C). Adding this

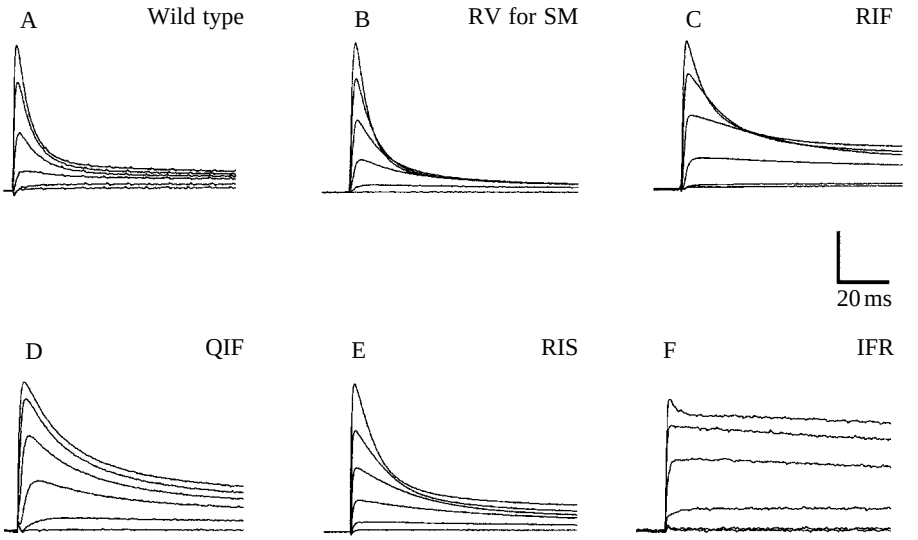

Fig. 2. Traces of currents expressed in *Xenopus laevis* oocytes, using two-electrode voltage-clamp, after injection of mRNA from the wild type (A) and from the S4 mutants RV for SM (B), RIF (C), QIF (D), RIS (E) and IFR (F). Recordings were made at room temperature (17–20 °C) 2–3 days after injection. Test pulses of 90 ms duration were given from a holding potential of −100 mV. Traces have been selected for each construct which best display the voltage sensitivities of the expressed current. These test pulses were as follows: for A, −30, −14, +6, +20, +44 and +66 mV; for B, −10, +6, +26, +46, +66 and +86 mV; for C, +15, +20, +60, +85, +110 and +135 mV; for D, −33, −12, +9, +30, +51 and +72 mV; for E, +66, +78, +90, +102, +114 and +126 mV; for F, −33, −12, +9, +30, +51 and +72 mV. The vertical current scale bar represents 1.2 μA in A, 2.2 μA in B, 2.1 μA in C, 0.64 μA in D, 2.4 μA in E and 0.8 μA in F.

seventh positively charged motif to the S4 region of *jShak1* produced a large positive shift (V_{50} +69 mV) in the activation curve relative to the wild type (P<0.001, Fig. 3) without altering the slope of the activation curve (Table 2). This mutant also showed a significant (P<0.001) positive shift in the mid-point (V_{50} +40 mV) of the steady-state inactivation curve without a significant increase in the slope of 5 mV/e (Fig. 4; Table 2). Thus, the threshold for activation is shifted in a positive direction without a large change in the activation slope.

QIF insertion

The QIF inserted mutant expressed a rapidly inactivating K^+ current (Fig. 2D), with a rate of inactivation (τ=15.7 ms) that was considerably slower than that of the wild type. The activation curve was shifted in a negative direction relative to the wild type (V_{50} +12 mV) with no significant difference (P=0.579) in the activation slope of 11 mV/e (Fig. 3; Table 2). The slope (9 mV/e) of the inactivation curve was unchanged relative to the wild type, and the mid-point of steady-state inactivation was not significantly (P=0.394) different from that of the wild type (Fig. 4; Table 2). Thus, increasing the length of the S4 segment by insertion cannot account for the voltage shifts that were seen when RIF was inserted.

RIS insertion

The RIS inserted mutant expressed a rapidly inactivating K^+

Table 2. *Biophysical properties of wild-type* jShak1, jShak2 *and the following S4 mutants of* jShak1*; RV for SM, RIF, QIF, RIS and IFR*

	jShak1	*jShak2*	RV for SM	RIF	QIF	RIS	IFR
Activation							
V_{50} (mV)	32.9±3.4 (8)	36.5±3.4 (3)	39.9±2.5 (8)	69.3±3.6 (5)	12.1±2.3 (5)	91.7±2.3 (5)	15.0±3.6 (5)
Slope (mV/e)	12.3±2.2 (8)	10.6±2.0 (4)	11.6±1.9 (8)	12.1±1.3 (5)	10.5±1.8 (5)	8.7±2.2 (5)	10.5±2.3 (4)
Inactivation							
V_{50} (mV)	−27.7±3.4 (8)	−7.4±5.6 (3)	−13.6±3.8 (5)	39.6±4.3 (5)	−23.1±2.3 (4)	57.9±1.4 (5)	9.04±3.3 (4)
Slope (mV/e)	8.5±1.6 (8)	5.7±4.3 (3)	6.0±1.5 (5)	5.3±2.4 (5)	8.7±1.4 (4)	5.1±2.2 (5)	8.4±1.5 (4)
τ (fast)	4.96±1.5 (5)	23.4±3.8 (3)	4.4±3.3 (5)	6.8±2.4 (5)	15.7±2.2 (4)	8.6±1.0 (5)	–

The V_{50} and slope (in mV per e-fold change in conductance) of activation and inactivation are derived from the Boltzmann fit of the conductance/voltage and steady-state inactivation data shown in Figs 3 and 4.

Limiting slopes were not calculated since certain mutants expressed currents that were not sufficiently large for reliable calculation of this parameter.

Values of τ for the fast components of inactivation were determined from the exponential fits of the major component of inactivation at test pulses of +70 mV for the wild type *jShak1*, *jShak2*, RV for SM, QIF, IFR and of +90 mV for RIF and RIS.

The inactivation parameters measured using the IFR mutant are for slow inactivation (presumably C-type); thus, the τ value for fast inactivation is not given.

Values are means ± S.E.M.; N is given in parentheses.

V_{50} is the voltage that gives half-maximal conductance; τ, time constant of inactivation.

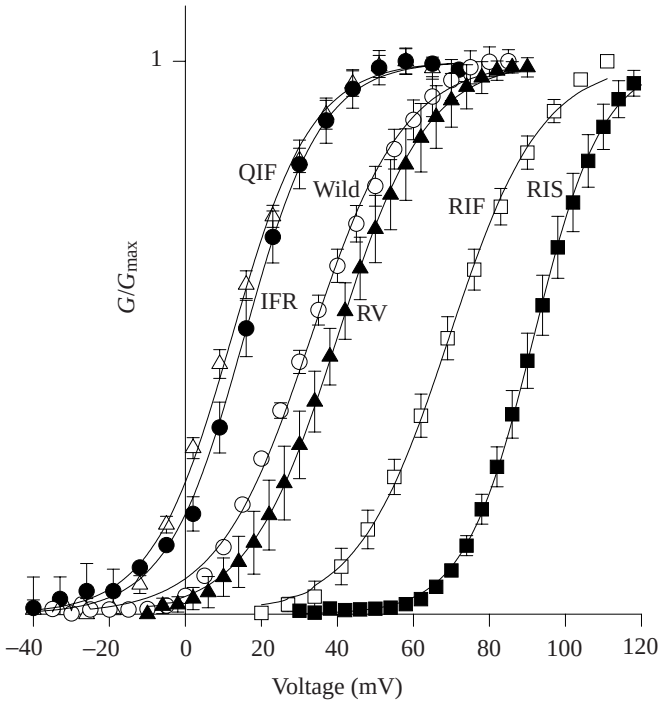

Fig. 3. Conductance/voltage curves for the wild type (open circles) and the S4 mutants RV for SM (RV; filled triangles), RIF (open squares), QIF (open triangles), RIS (filled squares) and IFR (filled circles). Recordings were made at room temperature (17–20°C) 2–3 days after injection. Test pulses of 90 ms duration were given from a holding potential of −100 mV. For each construct, the number of steps, the initial voltage step and the voltage increment of the test pulses were, respectively: wild type (25, −35 mV, 5 mV), RV for SM (26, −10 mV, 4 mV), RIF (14, +25 mV, 7 mV), QIF (17, −40 mV, 7 mV), RIS (23, 30 mV, +4 mV) and IFR (17, −40 mV, 7 mV). Peak currents were used to calculate conductances on the assumption that the reversal potential for all channels was −90 mV in ND 96. Unfortunately, very fast channel closing (<1 ms) did not allow us to measure the reversal potential from the tail currents. Normalized conductances were averaged for each trace and plotted against voltage. The data (± S.E.M., N as in Table 2) were fitted (solid curves) with a Boltzmann equation [$G/G_{max}=1/[1+\exp(-(V-V_{50})/a)]$], where G is the conductance at voltage V, G_{max} is the maximum conductance, V_{50} is the voltage at which $G=G_{max}/2$ and a is the slope factor.

current (Fig. 2E), with a rate of inactivation (τ=8.6 ms) that was slower than that of the wild type. This mutant produced the strongest positive shifts in both the activation curve (V_{50} +92 mV; Fig. 3; Table 2) and steady-state inactivation curve (V_{50} +58 mV; Fig. 4; Table 2), which were both significantly different (P<0.001) from values for the wild type. The slopes of activation and inactivation (9 mV/e and 5 mV/e respectively) were not significantly different (P=0.288 and P=0.298 respectively) from those of the wild type (Table 2). It appears that the lipophilic residue, phenylalanine, which was inserted with RIF, was also not responsible for the strong positive shifts in both activation and inactivation.

IFR insertion

When IFR was inserted between K294 and L295, this mutant expressed a current that lacked fast inactivation (Fig. 2F). Using longer test pulses, we were able to detect (data not shown) slow inactivation similar to that seen in an N-terminal deleted mutant, *jShak1T* [Δ1–23] (Jegla *et al.* 1995), which probably corresponds to a C-terminal inactivation process. It should be noted, however, that at very positive test potentials a small, fast inactivating component could be seen that indicates that a fast inactivating mechanism is still present. The activation curve was shifted significantly (P=0.005) in a negative direction relative to the wild type, with a mid-point of +15 mV, while the activation slope (11 mV/e) was not significantly changed (Fig. 3; Table 2). However, the mid-point of steady-state inactivation for this slow inactivation (–9 mV) was significantly (P<0.001) shifted to the right with a similar slope of 8 mV/e compared with the wild type (Fig. 4). This is the only mutant that showed shifts in the curves for

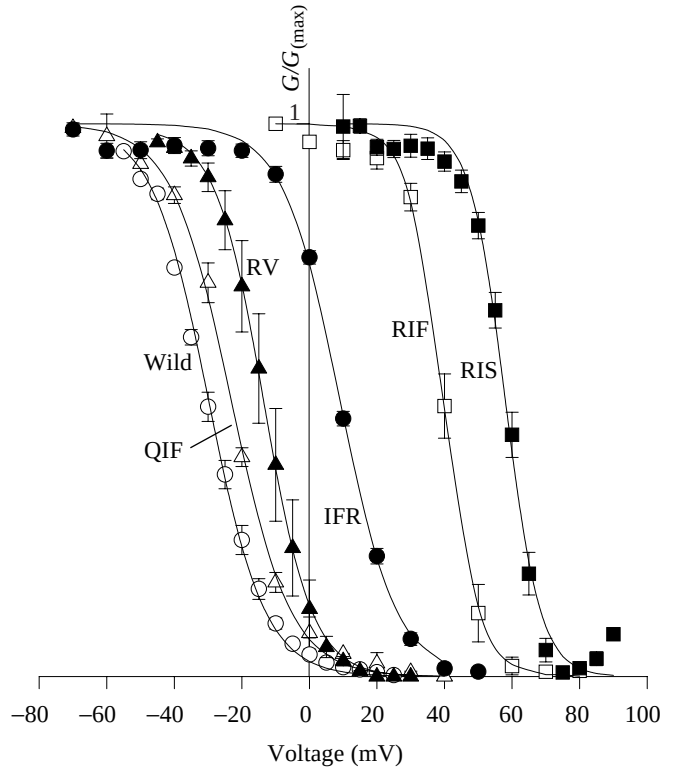

Fig. 4. Steady-state inactivation curves for the wild type (open circles) and the S4 mutants RV for SM (filled triangles), RIF (open squares), QIF (open triangles), RIS (filled squares) and IFR (filled circles). Recordings were made at room temperature (17–20 °C) 2–3 days after injection. Peak currents were measured using test pulses of 90 ms duration from a holding potential of −100 mV. Test pulses were preceded by 1 s prepulses to the voltages shown on the x-axis. The test pulse voltages were, respectively: wild type, RV for SM, IFR and QIF (+70 mV); RIF and RIS (+90 mV). Normalized conductances were averaged for each trace and plotted against voltage. The data (± S.E.M., N as in Table 2) were fitted (solid curves) with a Boltzmann equation [$G/G_{max}=1/[1+\exp(-(V-V_{50})/a)]$] where G is the conductance at voltage V, G_{max} is the maximum conductance, V_{50} is the voltage at which $G=G_{max}/2$ and a is the slope factor.

activation and steady-state inactivation that were in opposite directions.

IFQ insertion

Injected transcripts of the mutant IFQ (inserted between K294 and L295) failed to express any current. Unfortunately, we could not distinguish between a non-functional channel and lack of expression of the protein since no probes that could detect this protein were available.

Discussion

The appearance of multicellularity during evolution required that metazoan cells either modify the intracellular control mechanisms used by protists or evolve novel mechanisms for intercellular communication. As new physiological niches were opening up with the early radiation of the Metazoa, so were selective pressures increasing on voltage-gated (V_g) channels. That V_g K^+ channels must have diversified rapidly is indicated by the range of properties found in present examples of K^+ currents in the Cnidaria, a structurally and physiologically 'primitive' phylum (Anderson, 1989; Dunlap *et al.* 1987; Meech and Mackie, 1993*a*,*b*; Przysiezniak and Spencer, 1994).

Voltage-clamp recordings from excitable cells in a wide range of taxa have shown that the complement of K^+ channel types present is largely responsible for conferring the physiologically relevant excitability properties (Connor and Stevens, 1971; Rudy, 1988; Hille, 1992). Such properties include stabilization of the resting potential (inward rectifiers), regulation of action potential duration and expression of plateaux (delayed rectifiers), and regulation of firing frequency (A-like transient currents).

Data are scarce for the molecular structure of V_g K^+ channels in extant examples of the earliest metazoans, and we have only one example of protozoan K^+ channels. These protozoan channels from the ciliate *Paramecium tetraurelia* have very different deduced amino acid sequences from those of metazoans (Jegla and Salkoff, 1995; Jegla *et. al*. 1995; Chandy and Gutman, 1995), suggesting a different ancestry for ciliate channels or at least early diversification. Homologues of *Shal* and *Shaw*, as well as the *Shaker* homologues *jShak1* and *jShak2* described here, have been isolated from the cnidarian *Polyorchis penicillatus* (Jegla *et al.* 1995; T. Jegla, personal communication), indicating that the *Shaker* gene superfamily must have diversified early in metazoan evolution.

Despite being members of the same gene subfamily, *jShak1* and *jShak2* are structurally quite different in the S4 region. Like all other *Shaker* genes, *jShak2* has seven positively charged Arg/Lys-*X*-*X* motifs in S4, while *jShak1* has only six charged motifs. Despite this difference in charge, *jShak1* and *jShak2* have similar voltage sensitivities and voltage ranges (V_{50} of +33 mV and +37 mV, respectively), which are some 27–65 mV more positive than that of most other *Shaker* channels (Timpe *et al.* 1988; Pfaffinger *et al.* 1991; Chandy and Gutman, 1995). Although reductions of total positive charge in S4 can be correlated with decreases in gating valence (Logothetis *et al.* 1992, 1993), there is evidence that basic residues contribute unequally to gating valence and the threshold for activation (Tytgat *et al.* 1993; Papazian *et al.* 1991; Liman *et al.* 1991; Logothetis *et al.* 1992; Aggarwal and MacKinnon, 1996; Seoh *et al.* 1996). Because we had natural variants of S4 with differing charged motif content, we chose to investigate the effect of insertion or replacement of charged motifs. *jShak2*, with seven charged motifs, became a natural control for mutants of *jShak1* in which motifs were added.

When charge was added (RV for SM) to the N-terminal side of the S4 segment of *jShak1*, without altering the length of this segment, we did not observe any noticeable change in activation properties relative to the wild type. This suggests that the added charge created by the RV for SM mutation is outside the membrane voltage field and cannot participate in voltage sensing, which is consistent with experiments showing that the N terminus of S4 is on the extracellular side of the membrane (Manuzzu *et al.* 1996; Larsson *et al.* 1996). However, when R292 (the first arginine residue in S4) was neutralized in RCK1, giving a similar charge distribution to *jShak1*, a positive shift in the activation curve was seen when all four subunits were mutated (Tytgat *et al.* 1993).

All our remaining mutations, where motifs were inserted, caused elongation of the S4 segment. The increased length of S4 could be accommodated by displacement of the ends of the S4 segment either towards the cytoplasmic or extracellular surfaces or some combination of these movements. If insertion of RIF on the N-terminal side of K294 simply leads to this end of the S4 segment being displaced out of the membrane, then we can expect that the N-terminal residue of S4, namely R285, will not be a major contributor to voltage sensing. The RIF mutant would then have similar properties to the RV for SM mutant. This was not the case. The RIF insert produced large positive shifts in the activation and inactivation curves without substantially changing the slope of the activation curve. However, elongation alone could not have produced these depolarizing shifts in the activation and inactivation curves of the channel since the QIF mutation produced a negative shift in the activation curve while the inactivation curve of the channel was not significantly shifted. We conclude that the increase in length of the RIF insert does not interfere with the lateral electrostatic interactions between S4 and other transmembrane segments but may add mechanical constraints on S4 due to changes in length in a space that is limited by the location of the ends of S3 and S5. Therefore, a larger change in voltage is required for activation of the RIF mutant channel. However, the QIF mutation increases the length and eliminates a lateral salt bridge, thereby decreasing the activation threshold. We cannot rule out the possibility that the differences in charge act synergistically with other factors, such as hydrogen bond formation between S4 and other transmembrane elements.

The only *jShak1* mutant to show uncoupling of the voltage sensitivity of activation and inactivation was the IFR insert on the C-terminal side of K294. Interestingly, this mutant also

lacked fast inactivation, resembling a previously reported mutant, *jShak1T*, in which the N-terminal 23 amino acid residues were truncated (Jegla *et al.* 1995). It is likely that insertion of an additional motif on the C-terminal side of K294 causes an increase in the length of the S4–S5 loop which interferes with the interaction between the N-terminal inactivation peptide and the putative receptor on this loop (Isacoff *et al.* 1991). Therefore, the apparent uncoupling seen in IFR may be due to the different voltage-dependencies of steady-state fast inactivation and an unmasked slow C-terminal inactivation.

The marked differences seen when inserting the same set of residues (RIF or IFR) either before or after K294 can be explained by assuming that this lysine residue forms a salt bridge with acidic residues in adjacent segments and plays a critical role in protein folding, as demonstrated by Papazian *et al.* (1995) in *Shaker* B. We assume that K294 and R297 in *jShak1* are functionally equivalent to K374 and R377 in *Shaker* B (Papazian *et al.* 1991, 1995). Thus, interactions between K294 and other charged residues in *jShak1* appear to constrain movements of S4 by forming a fixed point.

Larsson *et al.* (1996) proposed that only one positively charged residue, R365, is buried in the membrane in the closed state and that, upon activation, four positively charged residues (R368–R377), which were previously intracellular, come to lie in the membrane. The results from two of our mutations support this model. First, addition of a charge to the N terminus of S4 by rewriting did not alter either valence or threshold. Second, when serine substituted for phenylalanine (RIS mutant) and charge is once again added on the N-terminal side of K294, there is an enormous shift (mean +72 mV) in both the activation and inactivation curves relative to the wild type. From this shift, we assume that the inserted serine residue must lie outside the membrane in the closed state and must move into a hydrophobic environment during activation. Since serine is far more polar than phenylanine, it will resist movement of the C-terminal end of the S4 segment into the membrane during activation.

An alternative model for voltage sensing has been proposed (Sigworth, 1994; Aggarwal and MacKinnon, 1996) in which the S4 segment is completely cytoplasmic in the closed state. This model cannot be reconciled with the structure of the two jellyfish *Shaker* channels since the loop connecting the S3 and S4 segments in both *jShak1* and *jShak2* is too short to span the membrane in the closed state. On the basis of the structural studies of Larsson *et al.* (1996) and those of Mannuzzu *et al.* (1996) and on the structural constraints implied by the sequences of *jShak1* and *jShak2*, it seems likely that the S4 segment spans the plasma membrane.

Papazian *et al.* (1995) have suggested that K374 and R377 participate in the formation of networks with acidic residues in segments S2 and S3 that stabilise the three-dimensional structure of the channel protein. It is interesting that *jShak1* has a pair of acidic residues (E237 and D260) in S2 and S3 in positions that align with those found in *Shaker* B (E293 and D316). However, a third acidic residue at E283 in *Shaker* B is replaced by asparagine in *jShak1* (N227) and *jShak2* (N225). It is possible that these asparagine residues are responsible for the difference between the activation thresholds of jellyfish *Shaker* channels when compared with other *Shaker* channels since neutralization of E283 in *Shaker* B shifted the activation curve by +78 mV (Papazian *et al.* 1995).

Although there has been considerable specialization of voltage-gated K^+ channels, many of the underlying mechanisms for sensing a voltage field have been conserved. This comparative approach allows us to separate specializations from the essential, shared functional properties.

We are very grateful to the staff of Bamfield Marine Station for their assistance in collecting animals. We thank Diane Papazian for her valuable comments. This study was supported by Natural Sciences and Engineering Research Council (Canada) Research Grants to A.N.S. and to W.J.G. J.D.S is the recipient of an Alberta Heritage Foundation for Medical Research Graduate Scholarship.

References

AGGARWAL, S. K. AND MACKINNON, R. (1996). Contribution of the S4 segment to gating charge in the *Shaker* K^+ channel. *Neuron* **16**, 1169–1177.

ANDERSON, P. A. V. (1989). Ionic currents of the Scyphozoa. In *Evolution of the First Nervous Systems* (ed. P. A. V. Anderson), pp. 267–280. New York: Plenum Press.

BAUMANN, A., GRUPE, A., ACKERMANN, A. AND PONGS, O. (1988). Structure of the voltage-dependent potassium channel is highly conserved from *Drosophila* to vertebrate central nervous systems. *EMBO J.* **7**, 2457–2463.

CHANDY, K. G. AND GUTMAN, G. A. (1995). Voltage-gated potassium channel genes. In *Handbook of Receptors and Channels: Ligand and Voltage-Gated Ion Channels* (ed. R. A. North), pp. 1–71. Boca Raton, FL: CRC Press.

CONNOR, J. A. AND STEVENS, C. F. (1971). Prediction of repetitive firing behaviour from voltage-clamp data on an isolated neuron soma. *J. Physiol., Lond.* **213**, 31–53.

DUNLAP, K., TAKEDA, K. AND BREHM, P. (1987). Activation of a calcium-dependent photoprotein by chemical signalling through gap junctions. *Nature* **325**, 60–62.

GREENBLATT, R. E., BLATT, E. AND MONTAL, M. (1985). The structure of the voltage-sensitive sodium channel. Inferences from computer-aided analysis of the *Electrophorus electricus* channel primary structure. *FEBS Lett.* **193**, 125–134.

HENGEN, P. N. (1995). Mini-prep plasmid DNA isolation and purification using silica-based resins. In *Molecular Biology: Current Innovations and Future Trends* (ed. H. Griffin), pp. 39–50. Wymondham, UK: Horizon Scientific Press.

HILLE, B. (1992). *Ionic Channels of Excitable Membranes.* Sunderland, MA: Sinauer.

ISACOFF, E. Y., JAN, Y. N. AND JAN, L. Y. (1991). Putative receptor for the cytoplasmic inactivation gate in the *Shaker* K^+ channel. *Nature* **353**, 86–90.

JEGLA, T., GRIGORIEV, N., GALLIN, W. J., SALKOFF, L. AND SPENCER, A. N. (1995). Multiple *Shaker* potassium channels in a primitive metazoan. *J. Neurosci.* **15**, 7989–7999.

JEGLA, T. AND SALKOFF, L. (1995). A multigene family of novel K^+ channels from *Paramecium tetraurelia*. *Receptors & Channels* **3**, 51–60.

JOHANSEN, K., WEI, A. G., SALKOFF, L. AND JOHANSEN, J. (1990). Leech gene sequence homologues to *Drosophila* and mammalian *Shaker*-K^+ channels. *J. Cell Biol.* **111**, 60a.

KAMB, A., IVERSON, L. E. AND TANOUYE, M. A. (1987). Molecular characterization of *Shaker*, a *Drosophila* gene that encodes a potassium channel. *Cell* **50**, 405–413.

KIM, E., DAY, T. A., BENNETT, J. L. AND PAX, R. A. (1995). Cloning, characterization and functional expression of a *Shaker*-related voltage-gated potassium channel gene from *Schistosoma mansoni* (Trematoda: Digenea). *Parasitology* **110**, 171–180.

LARSSON, H. P., BAKER, O. S., DHILLON, D. S. AND ISACOFF, E. Y. (1996). Transmembrane movement of the Shaker K^+ channel S4. *Neuron* **16**, 387–397.

LIMAN, E. R., HESS, P., WEAVER, F. AND KOREN, G. (1991). Voltage-sensing residues in the S4 region of a mammalian K^+ channel. *Nature* **353**, 752–756.

LOGOTHETIS, D. E., KAMMEN, B. F., LINDPAINTNER, K., BISBAS, D. AND NADAL-GINARD, B. (1993). Gating charge difference between two voltage-gated K^+ channels are due to the specific charge content of their respective S4 residues. *Neuron* **10**, 1121–1129.

LOGOTHETIS, D. E., MOVAHEDI, S., SATLER, S., LINDPAINTNER, K. AND NADAL-GINARD, B. (1992). Incremental reductions of positive charge within the S4 region of a voltage-gated K^+ channel result in corresponding decreases in gating charge. *Neuron* **8**, 531–540.

MANNUZZU, L. M., MORONNE, M. M. AND ISACOFF, E. Y. (1996). Direct physical measurement of conformational rearrangement underlying potassium channel gating. *Science* **271**, 213–216.

MEECH, R. W. AND MACKIE, G. O. (1993*a*). Ionic currents in giant motor axons of the jellyfish, *Aglantha digitale*. *J. Neurophysiol.* **69**, 884–893.

MEECH, R. W. AND MACKIE, G. O. (1993*b*). Potassium channel family in giant motor axons of *Aglantha digitale*. *J. Neurophysiol.* **69**, 894–901.

NODA, M., IKEDA, T., KAYANO, T., SUZUKI, H., TAKESHIMA, H., KURASAKI, M., TAKAHASHI, H. AND NUMA, S. (1986). Existence of distinct sodium channel messenger RNAs in rat brain. *Nature* **320**, 188–192.

NODA, M., SHIMIZU, S., TANABE, T., TAKAI, T., KAYANO, T., IKEDA, T., TAKAHASHI, H., NAKAYAMA, H., KANAOAKE, Y., MINAMINO, N., KANGAWA, K., MATSUO, H., RAFTERY, M. A., HIROSE, T., INAYAMA, S., HAYASHIDA, S., MIYATA, T. AND NUMA, S. (1984). Primary structure of *Electrophorus electricus* sodium channel deduced from cDNA sequence. *Nature* **312**, 121–127.

PAPAZIAN, D. M., SCHWARTZ, T. L., TEMPEL, B. L., JAN, N. J. AND JAN, L. Y. (1987). Cloning of genomic and complementary DNA from *Shaker*, a putative potassium channel gene from *Drosophila*. *Science* **237**, 749–753.

PAPAZIAN, D. M., SHAO, X. M., SEOH, S., MOCK, A. F., HUANG, Y. AND WAINSTOCK, D. H. (1995). Electrostatic interactions of S4 voltage sensor in Shaker K^+ channel. *Neuron* **14**, 1293–1301.

PAPAZIAN, D. M., TIMPE, L. C., JAN, Y. N. AND JAN, L. Y. (1991). Alteration of voltage-dependence of *Shaker* potassium channel by mutations in the S4 sequence. *Nature* **349**, 305–310.

PEROZO, E., SANTACRUZ-TOLOZA, L., STEFANI, E., BEZANILLA, F. AND PAPAZIAN, D. M. (1994). S4 mutations alter gating currents of *Shaker* K channels. *Biophys. J.* **66**, 345–354.

PFAFFINGER, P. J., FURUKAWA, Y., ZHAO, B., DUGAN, D. AND KANDEL, E. R. (1991). Cloning and expression of an *Aplysia* K^+ channel and comparison with native *Aplysia* K^+ currents. *J. Neurosci.* **11**, 918–927.

PRZYSIEZNIAK, J. AND SPENCER, A. N. (1994). Voltage-activated potassium currents in isolated motor neurons from the jellyfish *Polyorchis penicillatus*. *J. Neurophysiol.* **72**, 1010–1019.

RUDY, B. (1988). Diversity and ubiquity of K channels. *Neuroscience* **25**, 729–749.

SCHREIBMAYER, W., LESTER, H. A. AND DASCAL, N. (1994). Voltage clamping of *Xenopus laevis* oocytes utilizing agarose-cushion electrodes. *Eur. J. Physiol.* **426**, 453–458.

SEOH, S. A., SIGG, D., PAPAZIAN, D. M. AND BEZANILLA, F. (1996). Voltage-sensing residues in the S2 and S4 segments of the *Shaker* K^+ channel. *Neuron* **16**, 1159–1167.

SIGWORTH. F. J. (1994). Voltage gating of ion channels. *Q. Rev. Biophys.* **27**, 1–40.

STAPPERT, J. AND KEMLER, R. (1992). Functional analysis of uvomorulin by site-directed mutagenesis and gene transfer into eukaryotic cells. In *Cell–Cell Interactions* (ed. B. R. Stevenson, W. J. Gallin and D. L. Paul), pp. 75–89. New York: Oxford University Press.

TEMPEL, B. L., JAN, Y. N. AND JAN, L. Y. (1988). Cloning of a probable potassium channel gene from mouse brain. *Nature* **332**, 837–839.

TEMPEL, B. L., PAPAZIAN, D. M., SCHWARTZ, T. L., JAN, Y. N. AND JAN, L. Y. (1987). Sequence of a probable potassium channel component encoded at *Shaker* locus of *Drosophila*. *Science* **237**, 770–775.

TIMPE, L. C., SCHWARTZ, T. L., TEMPEL, B. L., PAPAZIAN, D. M., JAN, Y. N. AND JAN, L. Y. (1988). Expression of functional potassium channels from *Shaker* cDNA in *Xenopus* oocytes. *Nature* **331**, 143–145.

TYTGAT, J., NAKAZAWA, K., GROSS, A. AND HESS, P. (1993). Pursuing the voltage sensor of a voltage-gated mammalian potassium channel. *J. biol. Chem.* **268**, 23777–23779.

WEI, A., JEGLA, T. AND SALKOFF, L. (1996). Eight potassium channel families revealed by the *C. elegans* genome project. *Neuropharmac.* **35**, 805–829.